4660 *Macromolecules* **2010**, *43*, 4660–4666
DOI: 10.1021/ma100259t

Macromolecules
ARTICLE

Crystallinity and Cooperative Motions of Cyclic Molecules in Partially Threaded Solid-State Polyrotaxanes

Aoi Inomata,*,† Yasuhiro Sakai,† Changming Zhao,†,‡ Christian Ruslim,‡ Yuya Shinohara,† Hideaki Yokoyama,† Yoshiyuki Amemiya,† and Kohzo Ito*,†

†*Department of Advanced Materials Science, Graduate School of Frontier Sciences, The University of Tokyo, 5-1-5 Kashiwanoha, Kashiwa, Chiba 277-8561, Japan, and* ‡*Advanced Softmaterials, Inc., Tokatsu Techno Plaza 603, 5-4-6 Kashiwanoha, Kashiwa, Chiba 277-0882, Japan*

Received February 3, 2010; Revised Manuscript Received April 14, 2010

ABSTRACT: We investigated the structure, thermal properties, and dynamics of polyrotaxane (PR), composed of poly(ethylene glycol) (PEG) and α-cyclodextrins (CDs), and PR derivatives comprising hydroxypropylated CDs, that is, hydroxypropylated PRs (HyPRs), in the solid state by using wide-angle X-ray scattering (WAXS), differential scanning calorimetry (DSC), and viscoelastic spectroscopy. It was observed that HyPRs with high chemical modification ratios show a WLF-type viscoelastic relaxation that can be ascribed to the cooperative segmental motion of several CD molecules, whereas HyPRs with a lower modification ratio and PR with a highly ordered packing structure of CDs do not exhibit any mechanical relaxation mode. A comparison between the relaxation temperatures of HyPRs with different modification and inclusion ratios suggested that the hydrogen bond between CDs primarily dominates the viscoelastic properties of solid-state PR. Our experimental results indicate a close relationship between the crystallinity and fluctuation of cyclic molecules in solid-state PR, which is the first evidence of the dynamic softening of the glassy state formed by assembled cyclic molecules in solid-state PR.

1. Introduction

Polyrotaxane (PR), which consists of cyclic molecules threaded onto a linear polymer chain by mechanical binding, has been studied extensively because of its potential application as a smart and stimuli-responsive material.[1−7] Cyclic molecules can slide and rotate retaining the spatial constraints on a polymer chain. The unique structure and dynamics of PR enable its application in various nanoscale molecular devices: molecular tubes,[8] insulated molecular wires,[9,10] molecular shuttles,[11] drug delivery systems,[12] and multivalent ligand systems.[13] We have previously reported on a novel gel called "topological gel" or "slide-ring gel (SR gel)" that has sliding cross-links among cyclic molecules in different PRs. SR gels demonstrate remarkable properties such as high extensibility and a great degree of swelling because of their movable cross-links.[14,15]

We particularly focus on PRs consisting of α-cyclodextrin (CD) and poly(ethylene glycol) (PEG) because of their facile synthesis and biocompatibility.[16−18] Another significant feature of PR is that 18 hydroxyl groups of CD allow the modification of the CD moiety by a variety of functional groups such as hydroxypropyl, methyl, and acetyl groups. Chemically modified PRs (i.e., PR derivatives) are capable of unique functions such as thermoresponsivity[19,20] and photoresponsivity[21] and of improved characteristics such as solubility in organic solvents.[22]

Recently, we reported peculiar PR derivatives that enable the possible application of PRs in solvent-free systems; a liquid crystalline polyrotaxane (LCPR) having mesogenic side chains on CDs behaves as a thermotropic liquid crystal.[23] We also synthesized a "sliding graft copolymer (SGC)," which has polymeric mobile side chains attached to CDs. It differs from usual graft copolymers in that linear poly-ε-caprolactone (PCL) side chains can slide along and rotate around the main chain. A cross-linked SGC film can be prepared by connecting the ends of the side chains to each other; it has been found to be an elastomeric film with scratch-resistant properties in the dry, solvent-free solid state.[24] In addition, a preparation of PR-cellulose hybrid fibers containing no solvent has achieved the high-tensile properties.[25] Accordingly, the structure and dynamics of PRs in solid-state materials has attracted great interest and raised the following questions: To what extent do CDs form an ordered structure in solid-state PR? Or else, is arrangement of CDs completely random? Can PEG chains in PR fluctuate with segmental motions in solid state or not? How do CDs slide and rotate in solid-state PR?

The microscopic sliding of CDs has been experimentally verified in PR solutions by small-angle neutron scattering (SANS),[26−29] small-angle X-ray scattering (SAXS),[30] nuclear magnetic resonance spectroscopy (NMR),[31,32] and quasi-elastic light scattering (QELS).[33] The conformation of PR at various concentrations has also been investigated by SANS.[34] In contrast, there have been few reports on PRs in the dry or solid state. Even though some previous studies investigated the kinetics of the formation of inclusion compounds in the solid state and the structure of CD stacks in solid-state PRs,[35−37] or the polymer chain dynamics within CD nanotubes,[38] few reports have focused on the material characteristics and dynamics in the whole system of a solid-state PR compared with conventional polymer solids. We recently reported on the dielectric relaxation spectra of PR and LCPR,[39] which reflect the local dynamics of CDs or the PEG backbone in PR.

In this study, we investigate the crystallinity of the packing structure for CDs in PR and PR derivatives in the solid state and the slow dynamics related to mechanical relaxation processes in

*Corresponding authors. E-mail: inomata@molle.k.u-tokyo.ac.jp (A.I.), kohzo@molle.k.u-tokyo.ac.jp (K.I.).

 Published on Web 04/27/2010 © 2010 American Chemical Society

solid-state PR. We use a series of hydroxypropylated PRs (HyPRs) as PR derivatives. The hydroxypropylation of PR weakens the hydrogen bonds between CDs and prevents aggregation of CDs in PR, which considerably improves the solubility of PR in various solutions, especially aqueous ones.[40,41] The hydroxypropylation of PR in the solid state should also reduce the interaction between CDs and hinder the packing structure of CDs similarly to when they are in a solution. The PRs and HyPRs used in this study have low coverage (inclusion) ratios of the chains by CDs. PRs sparsely including CDs have been used for various materials, including slide-ring gels,[14] and have attracted much attention for their potential applications because of their high degree of freedom in terms of the arrangement and mobility of CDs on the PEG chain.

2. Experimental Section

2.1. Materials. PR, consisting of PEG with a weight-average molecular weight of 35000, α-CD, and adamantanamine (Figure 1), was prepared by a previously reported method.[16] The product was purified by precipitation from hot ethanol followed by recrystallization with ethanol and vacuum-drying. Four types of hydroxypropylated PRs (HyPRs) listed in Table 1 were prepared by a method reported in the literature.[40,41] After hydroxypropylation of CDs, the sample was purified by dialysis against deionized water and then freeze-dried. The average number of CDs in a single PR chain was estimated to be about 110 by ^{1}H NMR analysis, which corresponds to an inclusion ratio of 28%. (One α-CD molecule can perfectly cover two PEG monomer units.)

HyPRs in this study have CDs partially chemically modified by hydroxypropyl (Hy) groups (Figure 1). The ^{1}H NMR analysis indicated that the four samples had different inclusion and modification ratios with Hy groups. The modification ratio represents how many hydroxyl groups on α-CD are substituted by Hy groups. For example, HyPR38-28 was named after a modification ratio of 38% and inclusion ratio of 28%; the modification ratio implies that ca. 6.8 Hy groups were introduced per CD.

For comparison with the crystalline structures of PR and HyPRs, commercial poly(ethylene glycol) (PEG35) with a molecular weight of 35000 (Fluka) was used in wide-angle X-ray scattering (WAXS) measurements without purification.

2.2. Wide Angle X-ray Scattering (WAXS). Wide angle X-ray scattering (WAXS) measurements were performed using an X-ray diffractometer Rigaku NANO-Viewer with Cu Kα (λ = 1.5418 Å) radiation from a confocal multilayer monochromator (45 kV, 60 mA). The diffraction patterns were recorded on Fuji Film BAS-MS 2025 imaging plates. Each powder sample was sandwiched between 0.07 mm thick polyimide films and placed in a Linkam TH600 hot stage attached to a Linkam PR600 thermal controller. The distance between the sample and detector was ca. 130 mm (calibrated with a Si 100 diffraction peak).

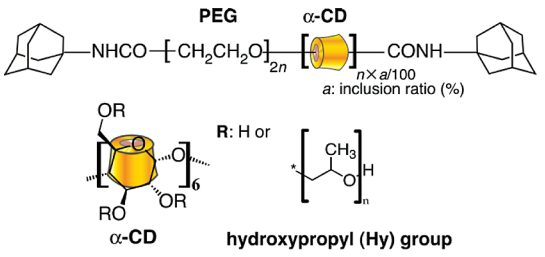

Figure 1. Chemical structure of PR and HyPRs.

2.3. Differential Scanning Calorimetry (DSC). Power-compensation DSC measurements were conducted using a Pyris Diamond DSC with a Cryofill liquid nitrogen cooling system (PerkinElmer, Inc.). Each sample was encapsulated in an aluminum pan and annealed at 100 °C in vacuum for 4 h before the measurement. Heating and cooling scans were carried out from −90 to 160 °C at a scanning rate of 20 K/min.

2.4. Dynamic Viscoelastic Measurements. Dynamic mechanical measurements were performed with a RSA III strain-controlled rheometer (TA Instruments) with parallel plate configuration. PR and PR derivative samples were pressed at 4.5 kbar at room temperature in vacuum to obtain pellets 13 mm in diameter. The thickness of the pellets ranged from 0.30 to 1.2 mm. Each pellet was annealed at 100 °C in vacuum for 4 h. All of the measurements were performed in compression mode under dried air in a frequency range between 0.06 and 100 rad/s; they took place within the linear response region at a certain fixed strain amplitude of 0.3 to 0.8% with respect to each sample. The measurement temperature ranged from 30 to 130 °C; the upper limit of the temperature range was kept under the oxidative degradation temperature for PEG (ca. 150 °C).

3. Results and Discussion

3.1. Crystalline Structures and Thermal Transitions. Figure 2 shows the WAXS profiles of PR, HyPRs, and PEG35 at room temperature: $q = 4\pi(\sin\theta)/\lambda$ is the magnitude of the scattering vector and 2θ is the scattering angle.

All profiles were largely different from that of α-CDs,[42] which form cage-type crystalline structures without guest molecules in the cavities. Strong diffraction peaks were observed for PR (Figure 2a) at q = 0.908, 1.39, and 1.58 Å^{-1}. Very similar diffraction patterns have been reported for PEG-CD inclusion complexes by some research groups.[43,44] The observed peaks in Figure 2a were assigned to 110, 210, and 300 reflections for the hexagonal lattice of CDs in a channel-type crystalline structure (Figure 3a) formed by hydrogen bonding between CDs. As shown in Figure 2, only reflections related to the regularity in the *ab*-plane of the hexagonal lattice were observed. This suggests that the arrangement of CD molecules along the *c*-axis is not highly ordered and that head-to-head packing arrangement of CDs in the *c*-axis cannot be formed in order because of the low inclusion ratio of CDs. Consequently, CD molecules in PR should be placed in hexagonally packed columns with a disordered arrangement in the *c*-axis, as depicted in Figure 3b. In contrast, PEG segments uncovered by CDs in PR form no crystalline structures by themselves because the WAXS profile of PR shows no crystalline peaks of pure PEG (Figure 2 f).

All WAXS profiles of the HyPR samples (Figure 2b−e) commonly show broad humps instead of the crystalline peaks observed in PR; these humps, or the so-called "amorphous halo,"[45] correspond to the average structural correlation distances. This indicates that chemically modified CDs in HyPRs do not form any crystalline structures with highly

Table 1. Unmodified Polyrotaxane (PR) and Hydroxypropylated PRs (HyPRs)

sample	functional group (−R)	modification ratio (%)	inclusion ratio (%)
PR	H (unmodified)	0 (unmodified)	28
HyPR38-28	$[CH_2CH(CH_3)O]_nH$	38 (6.8 groups/CD)	28
HyPR25-28	$[CH_2CH(CH_3)O]_nH$	25 (4.5 groups/CD)	28
HyPR78-21	$[CH_2CH(CH_3)O]_nH$	78 (14.0 groups/CD)	21
HyPR40-21	$[CH_2CH(CH_3)O]_nH$	40 (7.2 groups/CD)	21

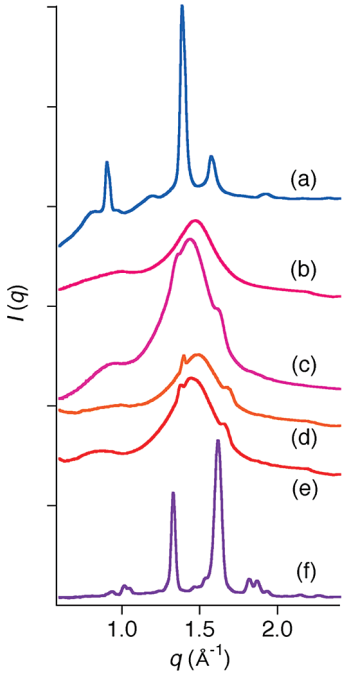

Figure 2. WAXS profiles of (a) PR, (b) HyPR25-28, (c) HyPR38−-28, (d) HyPR40-21, (e) HyPR78-21, and (f) PEG35.

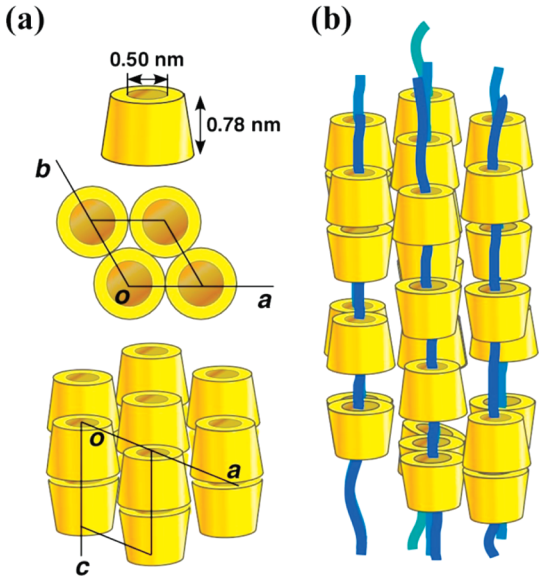

Figure 3. (a) Channel crystalline structure of α-CDs.[43] (b) Hexagonally packed columns formed by CDs in PR with disordered arrangement in the *c*-axis.

ordered packing; this is probably due to steric hindrance by the hydroxypropyl groups as well as interruption of intermolecular hydrogen bonding between the CD hydroxyl groups.

Small peaks were observed at $q = 1.35$ and 1.64 $Å^{-1}$; they overlapped the amorphous halo in the WAXS profiles of HyPR38-28, HyPR40-21, and HyPR78-21 (Figures 2c,d,e), respectively). These peaks correspond to the diffraction peaks observed for a crystalline structure[46] of pure PEG35 (Figure 2f). Accordingly, some parts of uncovered PEG segments in HyPRs seem to form a crystalline structure similar to pure PEG. In contrast, the diffraction pattern of HyPR25-28 (Figure 2b) did not have such crystalline peaks; interaction between CDs such as hydrogen bonds between

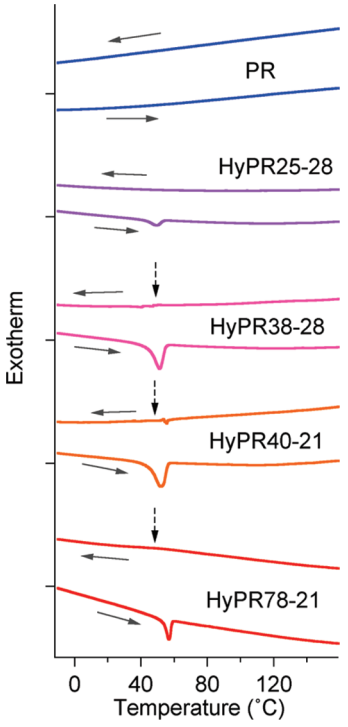

Figure 4. DSC traces (scanning rate: 20 K/min) of PR and HyPR samples. Solid arrows indicate the direction of the scans. Dashed arrows point toward the thermal transition points. The lower temperature limit of the graph is set at −10 °C for good legibility of the DSC profiles. No thermal transition was observed below −10 °C with the exception of the exothermic peak described below (Figure 5).

the unmodified hydroxyl groups in HyPR with a lower modification ratio may hinder the crystallization of PEG segments.

Figure 4 summarizes the DSC measurement results for PR and all of the HyPR samples. PR did not show any thermal transitions over the measured temperature range. PR seems to maintain the channel crystalline structure of CDs at temperatures below the oxidative degradation temperature of PEG.[35] In addition, there were no signs of melting and crystallization of PEG, although this can be observed at about 52 °C for pure PEG35.

DSC profiles for the cooling runs of HyPR38-28, HyPR40-21, and HyPR78-21 had slight baseline shifts, as illustrated by the dashed arrows. This behavior is similar to the glass transition of general amorphous polymers. Transition temperatures were evidently much higher than the glass-transition temperature[47] of pure PEG35 (ca. −51 °C): 49 °C for HyPR38-28 and 48 °C for both HyPR40-21 and HyPR78-21. For HyPR25-28, the above-mentioned thermal transition was not observed during the cooling run.

In addition, all of the HyPR samples showed endothermic peaks at 50−60 °C on the heating runs. Because the transition temperature was near the melting point of pure PEG, the transition should be due to the melting of the PEG crystalline domain in HyPRs. Curve (i) in Figure 5a represents the WAXS profile of HyPR78-21 heated at 100 °C. The diffraction peaks corresponding to the crystalline structure of PEG, which was observed at room temperature (Figure 2d), were found to disappear at 100 °C; they did not appear again even after the sample was cooled to 30 °C (Figure 5a (ii)). Upon further cooling to −50 °C (Figure 5a (iii)), the diffraction peak at $q = 1.64$ $Å^{-1}$ (indicated by a solid arrow) was again observed. In the cooling process to −90 °C in the DSC measurement of HyPR78-21 (Figure 5b), an exothermic

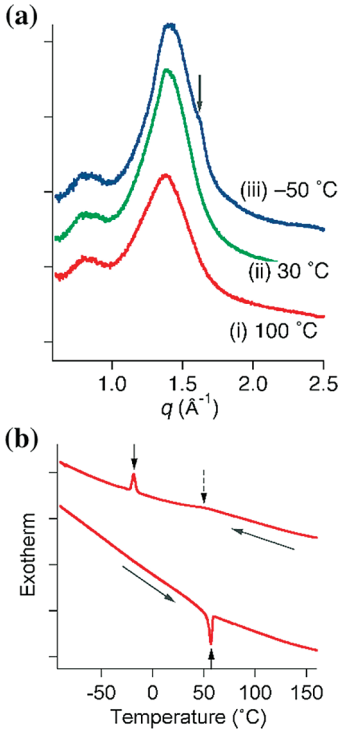

Figure 5. (a) WAXS profiles of HyPR78-21 (i) heated at 100 °C and cooled to (ii) 30 and (iii) −50 °C. The temperature of the sample was changed at the rate of 3 K/min. (b) DSC profile of HyPR78-21 from −90 to 160 °C at a scanning rate of 20 K/min. The dashed arrow points toward the same transition point, as shown in Figure 4.

peak was observed at −18 °C (indicated by a short solid arrow). On the basis of the WAXS measurement results, this exothermic peak should be ascribed to the crystallization of PEG in HyPR78-21. The crystallization temperature was far from the melting temperature; such a difference was not observed for pure PEG. This suggests that the formation of the PEG crystalline structure is substantially hindered by CDs in the inclusion complexes.

3.2. Viscoelastic Properties. The dynamic viscoelastic measurements of PR in the frequency and temperature ranges of 0.06 to 100 rad/s and 30 to 130 °C, respectively, showed no apparent relaxation process. Figure 6a shows the storage modulus $G'(\omega)$ and loss modulus $G''(\omega)$ at 120 °C as functions of the angular frequency of the strain input ω. G' of PR indicated almost no frequency dependence, and the value remained on the order of 10^7 (Pa) over the whole measured frequency range. Almost identical behavior was observed at different temperatures in the range of 30 to 130 °C. This behavior is consistent with the lack of thermal phase transitions (Figure 4) below the decomposition temperature in unmodified PR. HyPR25-28 also showed no apparent relaxation process in the measured frequency and temperature ranges (Figure 6b).

In contrast, HyPR38-28 clearly exhibited a viscoelastic relaxation process for the same frequency and temperature ranges; this is the first report of a viscoelastic relaxation process in solid-state PR. The data at different temperatures could be superimposed by shifting the angular frequencies. Figures 6c,d show the master curves of $G'(\omega)$ and $G''(\omega)$ at the reference temperature of 131 °C; they indicate the time−temperature superposition principle[48] for the complex modulus $G^* = G'(\omega) + G''(\omega)$

$$G^*(T,\omega) = G^*(T_0, a_T\omega) \quad (1)$$

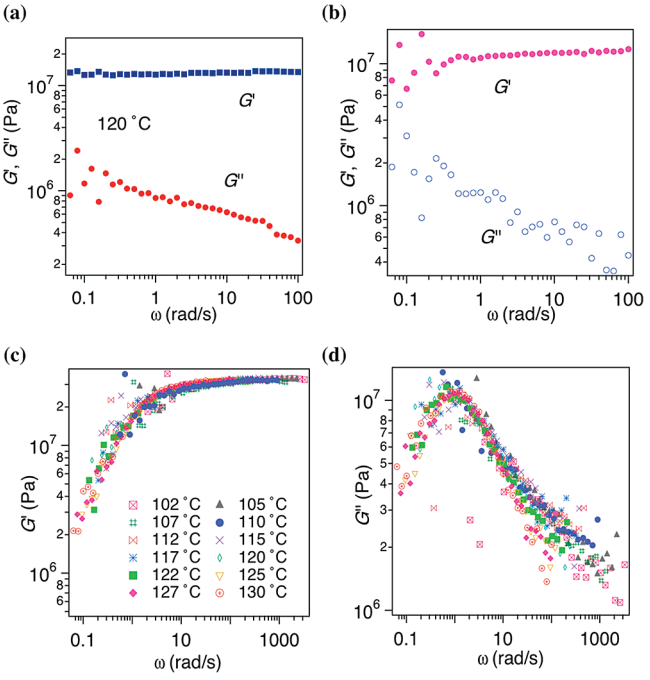

Figure 6. Storage and loss moduli of (a) PR at 120 °C and (b) HyPR25-28 at 120 °C. Master curves of (c) storage modulus and (d) loss modulus of HyPR38-28 are obtained at reference temperature of 131 °C.

where a_T represents the temperature shift factor that is the ratio of a relaxation time at the reference temperature T_0 to that at the measured temperature T. In this study, the temperature that gave the peak for $G''(\omega)$ at 1 rad/s was chosen as the reference temperature T_0 for each viscoelastic spectrum.

Because a systematic shift in the frequency range of the transition with temperature was observed, this transition is clearly ascribed to a kinetic phenomenon, such as the glass−rubber transition,[49] rather than a structural transition like the melting process or a solid−solid phase change. This transition should correspond to the thermal transitions observed in the DSC measurements (Figure 4). One significant feature was that the storage modulus, which was on the order of 10^7 Pa at low temperature, was much smaller than the typical moduli for glass polymers, which is on the order of 10^9 Pa.[50] However, we did not regard this relaxation process as a terminal relaxation in usual polymers because the value of the storage modulus at high temperature is much larger than that typical for polymers in the terminal flow range (normally smaller than 10^4 Pa);[50] in addition, no power-law dependence in the low-frequency region[51] was observed.

HyPR78-21 exhibited a similar viscoelastic relaxation process to that of HyPR38-28 but at considerably lower temperatures. Figure 7a,b shows the master curves of $G'(\omega)$ and $G''(\omega)$ at the reference temperature of 44 °C. HyPR40-21 also exhibited a viscoelastic relaxation process. The master curves of $G'(\omega)$ and $G''(\omega)$ at the reference temperature of 113 °C are shown in Figure 7c,d. Values of the storage moduli for all samples were on the same order as that of HyPR38-28.

For the viscoelastic relaxation processes of HyPR38-28, HyPR78-21, and HyPR40-21, the temperature dependences of the time-scale shift factors a_T (Figure 8) are well described by the empirical Williams−Landel−Ferry (WLF) equation, which is often used to analyze relaxation processes related to the dynamic glass transitions of amorphous polymers[52]

$$\log a_T = \frac{c_1(T - T_0)}{c_2 + (T - T_0)} \quad (2)$$

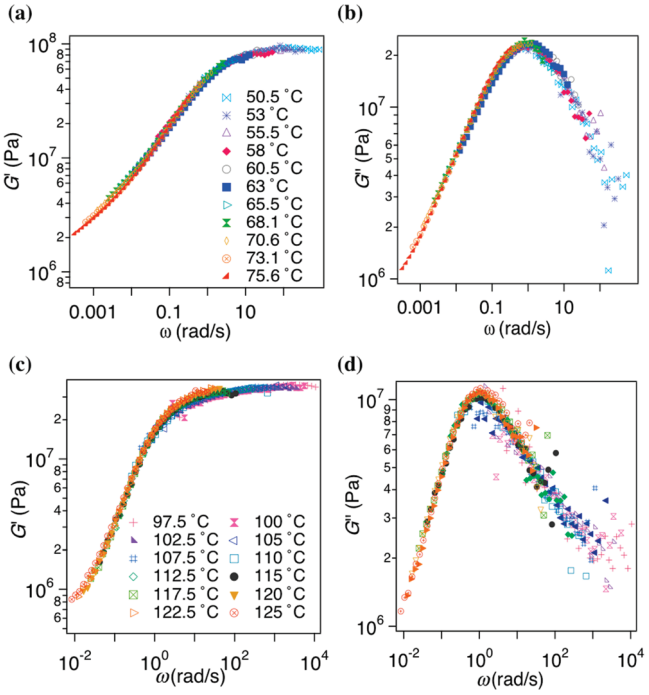

Figure 7. Master curves of (a) storage modulus and (b) loss modulus of HyPR78-21 at reference temperature of 44 °C and of (c) storage modulus and (d) loss modulus of HyPR40-21 at reference temperature of 113 °C.

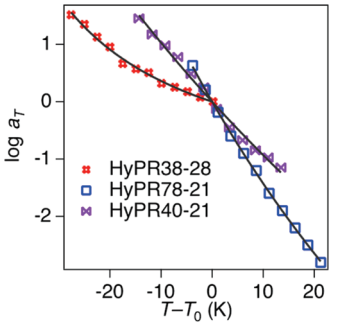

Figure 8. Logarithm plot of temperature dependence of time-scale shift factor for HyPR38-28, HyPR78-21, and HyPR40-21. The solid curves are the best-fitting ones obtained by eq 2.

where c_1 and c_2 are the empirically determined constants, which are related to the free volume of the polymer at the reference temperature T_0.

The fitting parameters are summarized in Table 2. All of the parameter values are comparable to those of viscoelastic relaxation processes corresponding to the glass transitions or dynamic softening transitions of ordinary polymers,[50,53] but they are somewhat different from each other.

The relaxation processes observed in the three kinds of HyPRs (HyPR38-28, HyPR78-21, and HyPR40-21) are considered here. Because all of the processes exhibited a WLF-type temperature dependence, each process should be equivalent to a primary dispersion that is related to the glass transition of conventional polymers, that is, the cooperative segmental motion in polymer chains. This mechanism is consistent with the thermal properties commonly observed in DSC experiments. Because hydroxypropylated CD has the largest weight fraction (CD/PEG = ca. 3.1:1 by weight in PR under a coverage ratio of 28%) among the components of each HyPR, displacement of CD molecules should most affect the deformation of HyPR samples. Local fluctuations

Table 2. Fitting Parameters Obtained by WLF Equation (eq 2)[a]

sample	T_0 (K)	c_1	c_2
HyPR38-28	404	1.77	58.9
HyPR78-21	327	18.1	117
HyPR40-21	386	20	204

[a] Reference temperature, T_0, is associated with the peak for G'' at 1 rad/s.

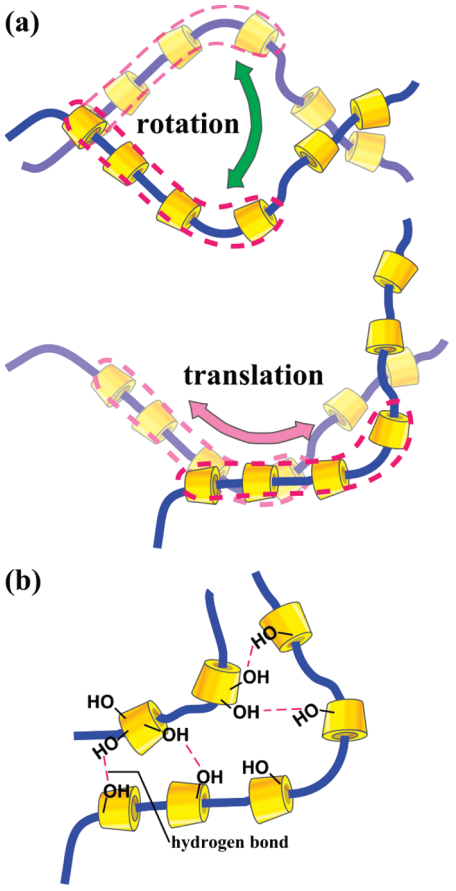

Figure 9. (a) Molecular fluctuation of CDs related to viscoelastic relaxation processes in HyPRs. (b) Hydrogen bonds between residual hydroxyl groups of HyPR25-28.

such as a rotational motion of hydroxypropyl groups on CDs or a plain rotation of a single CD molecule around the cavity axis can barely produce macroscopic strain. Even if PEG segments solely fluctuate without displacement of CDs, HyPR samples will be deformed slightly. In addition, the cooperative segmental motion in an amorphous domain of pure PEG occurs at significantly lower temperatures[54] than the relaxation processes of HyPRs in this study. Therefore, the viscoelastic relaxation process commonly observed in the three types of HyPR can be ascribed to the cooperative motion of several CD molecules constrained on the PEG chain (Figure 9a), that is, rotational or tranlational (sliding) motion of a string of several CD molecules.

In contrast, PR and HyPR25-28 did not exhibit any viscoelastic relaxation processes in the measured frequency and temperature ranges. The absence of a relaxation process is consistent with the results from the WAXS and DSC experiments: PR had no thermal transition, and the columnar crystal structure of CDs was maintained below the decomposition temperature.[35] Unlike other HyPR samples, HyPR25-28 did not show a relaxation process despite the lack of a crystalline packing structure for CDs. It is possible

Table 3. Crystallinity and Viscoelastic Relaxation Process of PR and HyPRs

sample	modification (%)	inclusion (%)	structure	viscoelastic relaxation
PR	0	28	columnar crystal of CD, PEG: amorphous	no relaxation
HyPR38-28	38	28	CD: amorphous, PEG: slightly crystalline	404 K (1 rad/s)
HyPR25-28	25	28	CD: amorphous, PEG: amorphous	no relaxation
HyPR78-21	78	21	CD: amorphous, PEG: slightly crystalline	327 K (1 rad/s)
HyPR40-21	40	21	CD: amorphous, PEG: slightly crystalline	386 K (1 rad/s)

that the residual hydroxyl groups on CDs in HyPR25-28 formed hydrogen bonds with each other (Figure 9b) or had any other attractive interaction (e.g., hydrophilic/hydrophobic interactions, van der Waals forces, or electrostatic interactions) because of the low chemical modification ratio, which hindered the molecular fluctuations of CDs.

The difference in the relaxation temperature range among the three HyPR samples is now considered. The reference temperature T_0 corresponding to the peak in $G''(\omega)$ of HyPR40-21 was about 18 K lower than T_0 for HyPR38-28. This indicates that a low inclusion ratio may simply assist in softening HyPR because these two samples have almost the same modification ratio and different inclusion ratios. In contrast, the HyPR78-21 T_0 was about 59 K lower than that of HyPR40-21. These two samples had different modification ratios. The considerably high modification ratio of HyPR78-21 should produce steric hindrance, which resulted in the reduction of the CD molecular interactions and the drastic lowering of the relaxation temperature. This indicates again that the interaction such as the hydrogen bond between CDs is an important factor that dominates the viscoelastic properties of solid-state PR.

As mentioned before, the storage moduli of the three HyPRs below the transition temperatures were on the order of 10^7 (Pa), which is much smaller than those of conventional polymers in a glassy state. The uncovered PEG segments in the rubber state at the HyPR transition temperatures may have decreased the elastic modulus of HyPRs. This effect was also found in PR and HyPR25-28, which have small storage moduli despite the crystalline structure and lack of a glass−rubber transition.

Additionally, solid-state PRs may have resemblance to glass-forming colloidal suspensions where the volume fraction of particles affects the viscosity of the system.[55] In HyPRs, CD crowding may have restricted the structural relaxation, inducing a glassy state. According to Figure 8 and Table 2, three HyPRs can be regarded as having different "fragility,"[56] that is, temperature sensitivity, from each other. HyPR78-21 seems to be most "fragile" among the three samples. There are several possible factors influencing on the fragility of HyPRs: deformability and elasticity of chemically modified CD cores, as well as interactions between CD cores. Further studies on the molecular dynamics of solid-state PRs using PRs with largely different inclusion ratios for example, may provide valuable information on glass formation phenomena.

The crystallinity and viscoelastic properties of PR and HyPRs are summarized in Table 3. Chemical modification of CDs in solid-state PRs significantly changed the CD molecular interactions such as hydrogen bonding and the PR characteristics in the solid state as well as in the solution.

PR maintained the columnar crystal structure of CDs and does not show a viscoelastic relaxation below the decomposition temperature. In contrast, HyPR38-28, HyPR78-21, and HyPR40-21 had disordered packing structures of chemically modified CDs. These HyPRs indicated viscoelastic relaxation processes corresponding to the dynamic softening of the glassy CD domains. The temperature ranges of the viscoelastic relaxations of HyPRs were different from each other; as the molecular interaction of CDs became weaker because of the steric hindrance by bulky hydroxypropyl groups, the viscoelastic relaxation temperature decreased. HyPR25-28 seemed to have stronger CD interactions than other HyPRs because of the weak steric hindrance. Then molecular interactions such as hydrogen bonds or van der Waals forces ought to be maintained below the decomposition temperatures.

Crystallinity of PEG exhibited a subtle difference depending on the molecular interaction of CDs; in PR and HyPR25-28, CDs tended to have strong interaction, and PEG had no crystallinity. Contrastively, in other HyPRs with weak molecular interaction of CDs, PEG slightly indicated the crystalline diffraction peak in the WAXS profile. However, the major part of PEG in these HyPRs is in the amorphous state. It has been found by dielectric relaxation measurements[57] that the molecular fluctuations in the amorphous domain of PEG occur in PR and HyPR in the temperature range of the viscoelastic measurements. It appears that PEG does not have a restraining effect on the viscoelastic relaxation in the whole system of HyPRs.

Here we report the first example of a cooperative segmental motion of CDs occurring in chemically modified PRs in the solid state and that the CD substituent and inclusion ratios significantly affect the molecular fluctuations in solid-state PR. For further studies, other experimental techniques that measure selectively the motion of individual molecular moieties may be effective for validation of the molecular mechanism of the molecular motions in solid-state PRs. We are currently carrying out solid-state NMR experiments on PR and HyPR in the equivalent temperature range as the viscoelastic measurements in this study.

4. Conclusions

We investigated the crystalline structure and thermal and viscoelastic properties of PR, consisting of PEG and CD, as well as that of PR derivatives, that is, HyPR containing chemically modified CDs with hydroxypropylated groups in the solid state. In the unmodified PR, CDs formed a hexagonally packed columnar structure with high regularity in a transverse direction through hydrogen bonds between the hydroxyl groups, whereas the series of HyPRs had a disordered packing of chemically modified CDs with bulky side groups. In the DSC measurements, thermal behavior similar to the glass transitions of conventional polymers were commonly observed for HyPRs with high modification ratios. We found that viscoelastic relaxation processes occur in HyPRs, which showed thermal transitions in the DSC measurements, in the solid state. These are the first evidence of the cooperative slow dynamics of cyclic molecules in solid-state PR. The relaxation processes exhibited WLF-type temperature dependences, which were ascribed to the cooperative rotational or translational motions of several CD molecules constrained on the PEG chain. The relaxation temperature of HyPRs depended on the CD inclusion and modification ratios. This suggested that the CD molecular interactions (hydrogen bonding, hydrophilic/hydrophobic interactions, van der Waals forces, or electrostatic interactions) should dominate the viscoelastic properties of solid-state PR. In contrast, the unmodified PR and HyPR with a lower

modification ratio did not show a relaxation process in the measured temperature and frequency ranges. The chemical structure of CDs in PR significantly affects the CD molecular interactions and physical properties of PR in the solid state as well as in the solution.

Our findings provide fundamental information on PRs in the solid state and will bring significant benefits to application studies of PRs in solvent-free systems. The structure and dynamics of PRs with different chemical structures, for example, PRs consisting of poly(dimethylsiloxane) and γ-cyclodextrin,[58] will also provide a new research perspective on PRs in the solid state.

Acknowledgment. This study was partially supported by the Ministry of Education, Science, Sports and Culture, Japan (Grant-in Aid for Scientific Research on Priority Areas, 2006-2010, no. 18068004) and Grant-in-Aid for Scientific Research ((S), 2008-2012, no. 20221005). We thank Ms. Michiko Ito (Advanced Softmaterials, Inc.) for supplying the PR derivative samples. We are grateful to Dr. Toshikazu Miyoshi (National Institute of Advanced Industrial Science and Technology) for fruitful discussions. A.I. also appreciates the financial support by a Grant-in-Aid for JSPS Fellows.

References and Notes

(1) Harada, A. *Coord. Chem. Rev*. **1996**, *148*, 115–133.
(2) Wenz, G.; Han, B. -H.; Müller, A. *Chem. Rev*. **2006**, *106*, 782–817.
(3) Gibson, H. W.; Bheda, M. C.; Engen, P. T. *Prog. Polym. Sci*. **1994**, *19*, 843–945.
(4) Huang, F.; Gibson, H. W. *Prog. Polym. Sci*. **2005**, *30*, 982–1018.
(5) Fleury, G.; Schlatter, G.; Brochon, C.; Hadziioannou, G. *Polymer* **2005**, *46*, 8494–8501.
(6) Takata, T; Kihara, N.; Furusho, Y. *Adv. Polym. Sci*. **2004**, *171*, 1–76.
(7) Raymo, F. M.; Stoddart, J. F. *Chem. Rev*. **1999**, *99*, 1643–1663.
(8) Harada, A.; Li, J.; Kamachi, M. *Nature* **1993**, *364*, 516–518.
(9) Cacialli, F.; Wilson, J. S.; Michels, J. J.; Daniel, C.; Silva, C.; Friend, R. H.; Severin, N.; Samori, P.; Rabe, J. P.; O'Connell, M. J.; Taylor, P. N.; Anderson, H. L. *Nat. Mater*. **2002**, *1*, 160–164.
(10) Shimomura, T.; Akai, T.; Abe, T.; Ito, K. *J. Phys. Chem*. **2002**, *116*, 1753–1756.
(11) Harada, A.; Hashidzume, A.; Takashima, Y. *Adv. Polym. Sci*. **2006**, *201*, 1–43.
(12) Ooya, T.; Yui, N. *J. Controlled Release* **1999**, *58*, 251–269.
(13) Ooya, T.; Eguchi, M.; Yui, N. *J. Am. Chem. Soc*. **2003**, *125*, 13016–13017.
(14) Okumura, Y.; Ito, K. *Adv. Mater*. **2001**, *13*, 485–487.
(15) Ito, K. *Polym. J*. **2007**, *39*, 489–499.
(16) Araki, J.; Zhao, C.; Ito, K. *Macromolecules* **2005**, *38*, 7524–7527.
(17) Araki, J.; Ito, K. *J. Polym. Sci., Part A: Polym. Chem*. **2006**, *44*, 532–538.
(18) Samitsu, S.; Araki, J.; Kataoka, T.; Ito, K. *J. Polym. Sci., Part B: Polym. Phys*. **2006**, *44*, 1985–1994.
(19) Kidowaki, M.; Zhao, C.; Kataoka, T.; Ito, K. *Chem. Commun*. **2006**, 4102–4103.
(20) Kataoka, T.; Kidowaki, M.; Zhao, C.; Minamikawa, H.; Shimizu, T.; Ito, K. *J. Phys. Chem. B* **2006**, *110*, 24377–24383.
(21) Sakai, T.; Murayama, H.; Nagano, S.; Takeoka, Y.; Kidowaki, M.; Ito, K.; Seki, T. *Adv. Mater*. **2007**, *19*, 2023–2025.
(22) Araki, J.; Ito, K. *Soft Matter* **2007**, *3*, 1456–1473.
(23) Kidowaki, M.; Nakajima, T.; Araki, J.; Inomata, A.; Ishibashi, H.; Ito, K. *Macromolecules* **2007**, *40*, 6859–6862.
(24) Araki, J.; Kataoka, T.; Ito, K. *Soft Matter* **2008**, *4*, 245–249.
(25) Araki, J.; Kataoka, T.; Katsuyama, N.; Teramoto, A.; Ito, K.; Abe, K. *Polymer* **2006**, *47*, 8241–8246.
(26) Karino, T.; Okumura, Y.; Zhao, C.; Kataoka, T.; Ito, K.; Shibayama, M. *Macromolecules* **2005**, *38*, 6161–6167.
(27) Karino, T.; Shibayama, M.; Okumura, Y.; Ito, K. *Physica B* **2006**, *385*−*386*, 807–809.
(28) Shibayama, M.; Karino, T.; Domon, Y.; Ito, K. *J. Appl. Crystallogr*. **2007**, *40*, S43–S47.
(29) Fleury, G.; Schlatter, G.; Brochon, C.; Travelet, C.; Lapp, A.; Lindner, P.; Hadziioannou, G. *Macromolecules* **2007**, *40*, 535–543.
(30) Shinohara, Y.; Kayashima, K.; Okumura, Y.; Zhao, C.; Ito, K.; Amemiya, Y. *Macromolecules* **2006**, *39*, 7386–7391.
(31) Zhao, T.; Beckham, H. W. *Macromolecules* **2003**, *36*, 9859–9865.
(32) Ceccato, M.; Nostro, P. L.; Rossi, C.; Bonechi, C.; Donati, A.; Baglioni, P. *J. Phys. Chem. B* **1997**, *101*, 5094–5099.
(33) Zhao, C.; Domon, Y.; Okumura, Y.; Okabe, S.; Shibayama, M.; Ito, K. *J. Phys.: Condens. Matter* **2005**, *17*, S2841–S2846.
(34) Mayumi, K.; Osaka, N.; Endo, H.; Yokoyama, H.; Sakai, Y.; Shibayama, M.; Ito, K. *Macromolecules* **2008**, *41*, 6480–6485.
(35) Huang, L.; Allen, E.; Tonelli, A. E. *Polymer* **1998**, *39*, 4857–4865.
(36) Peet, J.; Rusa, C. C.; Hunt, M. A.; Tonelli, A. E.; Balik, C. M. *Macromolecules* **2005**, *38*, 537–541.
(37) Girardeau, T. E.; Zhao, T.; Leisen, J.; Beckham, H. W.; Bucknall, D. G. *Macromolecules* **2005**, *38*, 2261–2270.
(38) Girardeau, T. E.; Leisen, J.; Beckham, H. W. *Macromol. Chem. Phys*. **2005**, *206*, 998–1005.
(39) Inomata, A.; Ishibashi, H.; Nakajima, T.; Sakai, Y; Shimomura, T.; Ito, K. *Europhys. Lett*. **2007**, *79*, 66004.
(40) Ooya, T.; Yui, N. *Macromol. Chem. Phys*. **1998**, *199*, 2311–2320.
(41) Araki, J.; Ito, K. *J. Polym. Sci., Part A: Polym. Chem*. **2006**, *44*, 6312–6323.
(42) McMullan, R. K.; Saenger, W.; Fayos, J.; Mootz, D. *Carbohydr. Res*. **1973**, *31*, 211–227.
(43) Topchieva, I. N.; Tonelli, A. E.; Panova, I. G.; Matuchina, E. V.; Kalashnikov, F. A.; Gerasimov, V. I.; Rusa, C. C.; Rusa, M.; Hunt, M. A. *Langmuir* **2004**, *20*, 9036–9043.
(44) Harada, A.; Kamachi, M. *Macromolecules* **1990**, *23*, 2821–2823.
(45) Rabiej, S. *Fibres Text. East. Eur*. **2005**, *13*, 30–34.
(46) Backley, C. P.; Kovacs, A. J. *Colloid Polym. Sci*. **1976**, *254*, 695–715.
(47) Faucher, J. A.; Koleske, J. V.; Santee, E. R., Jr.; Stratta, J. J.; Wilson, C. W., III. *J. Appl. Phys*. **1966**, *37*, 3962–3964.
(48) Ferry, J. D. *Viscoelastic Properties of Polymers*, 3rd ed.; John Wiley & Sons: New York, 1980; Chapter 11, pp 264−320.
(49) Strobl, G. R. *The Physics of Polymers*, 2nd ed.; Springer-Verlag: NewYork, 1997; Chapter 5, pp 213−256.
(50) Chen, Q.; Matsumiya, Y.; Masubuchi, Y.; Watanabe, H.; Inoue, T. *Macromolecules* **2008**, *41*, 8694–8711.
(51) Krishnamoorti, R.; Giannelis, E. P. *Macromolecules* **1997**, *30*, 4097–4102.
(52) Williams, M. L.; Landel, R. F.; Ferry, J. D. *J. Am. Chem. Soc*. **1955**, *77*, 3701–3707.
(53) Pan, X.-D. *J. Polym. Sci., Part B: Polym. Phys*. **2004**, *42*, 2467–2478.
(54) Arisawa, K.; Tsuge, K.; Wada, Y. *Jpn. J. Appl. Phys*. **1965**, *4*, 138–147.
(55) Mattsson, J.; Wyss, H. M.; Nieves, A. F.; Miyazaki, K.; Hu, Z.; Reichman, D. R.; Weitz, D. A. *Nature* **2009**, *462*, 83–86.
(56) Angell, C. A.; Ngai, K. L.; McKenna, G. B.; McMillan, P. F.; Martin, S. W. *J. Appl. Phys*. **2000**, *88*, 3113–3157.
(57) Inomata, A.; Kidowaki, M; Sakai, Y.; Yokoyama, H.; Ito, K., in preparation.
(58) Kato, K.; Inoue, K.; Kidowaki, M; Ito, K. *Macromolecules* **2009**, *42*, 7129–7136.